

# Anodically Deposited MnO<sub>2</sub>/Stainless Steel Supercapacitor Electrode at Different Mass Loadings and Different Na<sub>2</sub>SO<sub>4</sub> Electrolyte Concentrations

Sameh Hassan\*, A. H. Khafagy, Dalia Usama

Physics Department, Faculty of Science, Menoufia University, Shebin El-Koom, Menoufia, Egypt

**Abstract** Manganese dioxide thin films are prepared by anodic potentiostatic electrochemical deposition on etched stainless-steel substrates as a single supercapacitor electrode. Effects of different mass loadings of 25, 50, 100 μg/cm<sup>2</sup> for manganese dioxide films deposited on stainless-steel current collector, and concentrations of Na<sub>2</sub>SO<sub>4</sub> electrolyte solution in the range, from 0.1 to 0.9 mole/L, on the specific capacitance of the developed electrode are investigated using the cyclic voltammetry, galvanostatic charging-discharging curves, and electrochemical impedance spectra. The highest specific capacitances (484.7, 483.4 and 481.1 F/g) are obtained at 20 A/g (or 0.5 mA/cm<sup>2</sup>) with the electrode having mass loading of 25 μg/cm<sup>2</sup> at 0.1, 0.3 and 0.7 mole/L of Na<sub>2</sub>SO<sub>4</sub> electrolyte concentrations, respectively. This paper gives new vision on the charge storage mechanism in manganese dioxide/stainless-steel film as an active supercapacitor electrode material, and its transition between the pseudo-capacitive and double layer behaviors as an effect to the mass loading of the manganese dioxide film, and Na<sub>2</sub>SO<sub>4</sub> electrolyte concentration.

**Keywords** Electrolyte concentration, MnO<sub>2</sub> film, Mass loading, Double layer, Pseudo-capacitive

## 1. Introduction

Supercapacitors are charge storage devices that received a lot of attention due to their high power density, excellent reversibility, and very long cycle life. Also, they deliver higher energy density than conventional capacitors and higher power density than batteries [1-3]. In the last decades, MnO<sub>2</sub> has attracted great attention in the field of supercapacitor energy storage applications due to its abundance and untotoxicity as compared with the toxic and expensive ruthenium oxide. The energy storage of MnO<sub>2</sub> is attributed to ion insertion/desertion within its surface depending on particle size, surface area and porosity [4-6]. MnO<sub>2</sub>, among the other transition metal oxides, is the most widely investigated for pseudocapacitors due to its high theoretical specific capacitance of 1370 F/g, relatively low cost, and environmental friendly nature [7-12]. Also, MnO<sub>2</sub> has been prepared by several different methods like, chemical precipitate [13], sol-gel [14], pyrogenation [15], mechanical grinding [16], hydrothermal synthesis [17], and electrochemical deposition [18]. It has been reported [17-20] that the electrochemical deposition method proved to be more effective for preparing MnO<sub>2</sub> nanostructures.

Electrochemical deposition of MnO<sub>2</sub> could be prepared via two approaches; anodic oxidation and cathodic reduction, where the cations Mn<sup>2+</sup> and anions MnO<sub>4</sub><sup>-</sup> (Mn<sup>7+</sup>) precursors are commonly used in them, respectively. Both of anodic oxidation and cathodic reduction can be manipulated by potentiostatic (PS) at constant potential as well as galvanostatic (GS) at constant current processes [17,21-25]. It is worth mentioning that both (PS) and (GS) techniques could be electrochemically employed to produce nanostructures as well as amorphous films of MnO<sub>2</sub> films.

In this work, the charge storage mechanism and its transition between pseudo-capacitive behavior and double layer behavior have been shown by studying the effects of different mass loadings, and concentration of Na<sub>2</sub>SO<sub>4</sub> electrolyte solution on the specific capacitance of single manganese dioxide pseudocapacitor electrode that are investigated using: the cyclic voltammetry, galvanostatic charging/discharging curves, and electrochemical impedance spectra (EIS) methods to get optimized electrode for supercapacitor application.

## 2. Experimental

Manganese dioxide films were electroplated anodically onto 2 cm<sup>2</sup> of 304-stainless-Steel (SS) substrates of thickness 0.175 mm as a working electrode in 0.25 mole/L manganese acetate tetrahydrate (CH<sub>3</sub>COO)<sub>2</sub> Mn.4H<sub>2</sub>O plating solution by potentiostatic (PS) method at 1 Volt at room temperature

\* Corresponding author:

sameh.hassan@science.menoufia.edu.eg (Sameh Hassan)

Received: Aug. 14, 2020; Accepted: Aug. 28, 2020; Published: Sep. 15, 2020

Published online at <http://journal.sapub.org/materials>

(29°C). The substrates were first etched in conc. H<sub>2</sub>SO<sub>4</sub> 98% for 30 minutes, and then rinsed thoroughly with distilled water and air dried. The mass loading of the electrode films was selected to be 25, 50 and 100 µg/cm<sup>2</sup>, and controlled by adjusting the total charge passed through the electrode during deposition process.

The electrochemical characterization of the electrodes was performed by using the conventional three electrode system through EC-Lab software of SP-150 potentiostat/galvanostat device in an electrochemical cell with MnO<sub>2</sub>/stainless steel substrate as a working electrode, Ag/AgCl (KCl saturated) as a reference electrode, and platinum wire as a counter electrode. The prepared films were tested as electrodes for supercapacitor in different concentrations of Na<sub>2</sub>SO<sub>4</sub> electrolyte 0.1, 0.3, 0.5, 0.7 and 0.9 mole/L (mole/L is abbreviated to M) using cyclic voltammetry (CV), galvanostatic charge-discharge (CD), and electrochemical impedance spectroscopy (EIS) measurements. CV tests were conducted in the potential range (0-1 V) with different scan rates of 10-100 mV/s, as well as, at different current densities ranging from 0.5-5 mA/cm<sup>2</sup> in a voltage window between 0 and 1 V for CD tests. Besides, EIS data were recorded using sine wave voltage of amplitude 10 mV and frequency range of 100 kHz-10 mHz.

### 3. Results and Discussion

#### 3.1. Galvanostatic Charge-Discharge

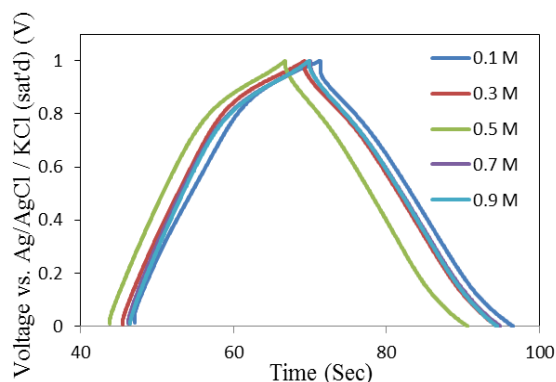


**Figure 1.** Galvanostatic CD curves for deposited MnO<sub>2</sub> electrodes at mass loading of 25 µg/cm<sup>2</sup>, measured at actual current 1 mA in different Na<sub>2</sub>SO<sub>4</sub> electrolyte concentrations

Galvanostatic charge-discharge is a reliable method for specific capacitance determination of supercapacitor electrodes by getting almost an exact value for the practical application. The electrochemical performance of the prepared electrodes was first characterized by galvanostatic charge-discharge curves using chronopotentiometry at actual charging currents from 1 - 10 mA with potential window between 0 and 1 Volt, for each concentration of Na<sub>2</sub>SO<sub>4</sub> electrolyte (0.1, 0.3, 0.5, 0.7 and 0.9 mole/L), and for the different mass loadings of MnO<sub>2</sub> films (25, 50 and 100 µg/cm<sup>2</sup>). Galvanostatic CD curves for 25 µg/cm<sup>2</sup> deposited mass of MnO<sub>2</sub> electrodes are shown in **Figure 1**,

measured at actual current 1 mA in different Na<sub>2</sub>SO<sub>4</sub> electrolyte concentrations as indicated.

As shown in **Figure 1**, the quasi-triangular shaped charge/discharge curves at current 1 mA for the deposited MnO<sub>2</sub> films indicate the capacitive characteristics of the tested MnO<sub>2</sub> electrodes. Moreover, these symmetrical charge/discharge curves prove the good capacitive property and reversibility of the electrochemical reactions in the MnO<sub>2</sub> films, which is in good agreement with the CV results (discussed later in this work).

Charge/discharge curves of **Figure 1** show for all investigated electrodes an evidence for a DC internal ohmic resistance exists at the voltage switching point. The variation of the calculated values of this DC internal resistance with the applied current densities for tested electrode with mass loading 25 µg/cm<sup>2</sup> is shown in **Figure 2**. The internal resistance slightly decreases as the current density increases for the same employed concentration. This common observed behavior is related to electrolyte ion mobility which increases as the current density increases.

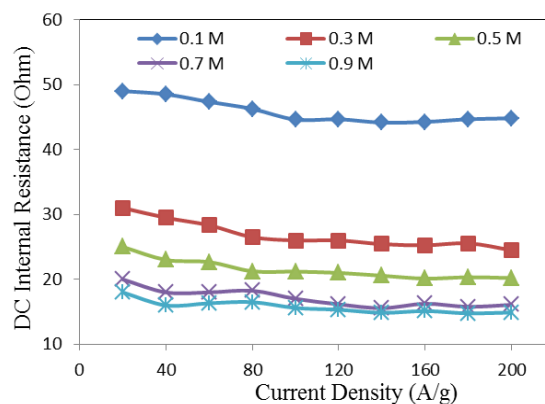


**Figure 2.** Variation of DC internal electrode resistance with current densities for electrode mass loading of 25 µg/cm<sup>2</sup>

Also, with respect to the internal resistance dependence on the electrolyte concentration, it is observed that, the resistance sharply decreases with the increase in Na<sub>2</sub>SO<sub>4</sub> electrolyte concentration up to 0.3 mole/L, and then showed more decreasing with a slower rate up to 0.9 mole/L, the end of tested concentration. This is occurred perhaps due to more ions accessibility to the electrode surface during their movement in the electrolyte as their numbers is increased upon increasing the concentration.

The values of specific capacitance SC were obtained from charge-discharge curves by using the following Equation (1):

$$SC = I dt / (m dv) \quad (1)$$

Where, I is the discharge current, m is the mass of the electrode film, and  $dv/dt$  is the slope of the discharge half cycle.

**Figure 3** shows the dependence of specific capacitance on current density for MnO<sub>2</sub> deposited films of mass loading 25 µg/cm<sup>2</sup>; as measured in different investigated electrolyte concentrations. From inspection of this Figure, it was observed that the SC gradually decreases as the current

density increases for all cases of investigated electrolyte concentrations keeping the level of SC values associated to lower concentration solution, 0.1 M is lower than that one's of higher concentrations especially at higher current density. This common decrease behavior can be attributed to the high accessibility of ions to the pores of electrode film surface at low charging rates. The highest specific capacitance value obtained for mass loading of  $25 \mu\text{g}/\text{cm}^2$  at 1 mA is 484.7 F/g at the corresponding  $\text{Na}_2\text{SO}_4$  electrolyte concentrations 0.1 mole/L, while that obtained for mass loading of  $50 \mu\text{g}/\text{cm}^2$  is 440.7 F/g at  $\text{Na}_2\text{SO}_4$  electrolyte concentrations 0.3 mole/L, and for mass loading of  $100 \mu\text{g}/\text{cm}^2$  is 386.7 F/g at  $\text{Na}_2\text{SO}_4$  electrolyte concentrations 0.5 mole/L.

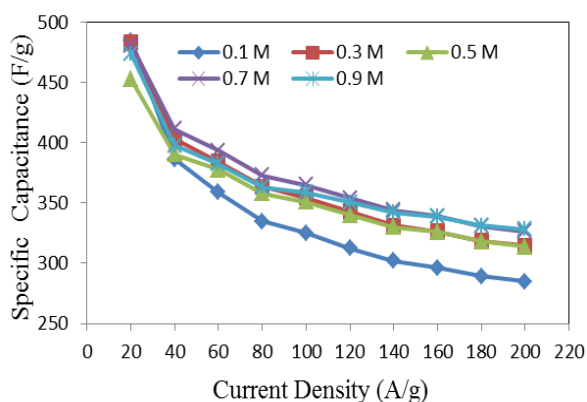


**Figure 3.** Variation of specific capacitance with current density for different  $\text{Na}_2\text{SO}_4$  electrolyte concentration at mass loading of electrode film  $25 \mu\text{g}/\text{cm}^2$

**Figure 4** presents the dependence of specific capacitance on  $\text{Na}_2\text{SO}_4$  electrolyte concentration for different mass loadings of electrode film (a) 25 (b) 50, and (c)  $100 \mu\text{g}/\text{cm}^2$  at different actual currents 1 to 10 mA. In general, the specific capacitance decreases with increasing mass loading of the  $\text{MnO}_2$  electrode because a large mass loading may cause lower electrical conductivity, limited access of electrolyte ions and higher series resistance due to longer transport paths for the diffusion of protons [26]. An interesting behavior was obtained in the variation of specific capacitance with  $\text{Na}_2\text{SO}_4$  electrolyte concentrations at each charging current for all mass loadings. For the electrode film of  $25 \mu\text{g}/\text{cm}^2$  loading, there are two maxima of SC values are observed at 0.3 and 0.7 mole/L around one minimum occurred at 0.5 mole/L of  $\text{Na}_2\text{SO}_4$  electrolyte concentrations. The optimized SC values (484.7, 483.4 and 481.1 F/g) were considered at 0.1, 0.3 and 0.7 mole/L at actual current 1 mA, respectively as shown in **Figure 4(a)**. While in case of electrode of mass loading  $50 \mu\text{g}/\text{cm}^2$ , it can be generally seen, the disappearance of the minimum at 0.5 mole/L in part (a) and the appearance of one maximum in the other parts (b) and (c) at the same concentration 0.5 mole/L for all currents, except for the low actual currents 1 and 2 mA in **Figure 4(b)**, the optimized SC values (440.7 & 370.1 F/g) were obtained at 0.3 mole/L, respectively, while the electrode of mass loading  $100 \mu\text{g}/\text{cm}^2$  showed the optimized SC value (386.7 F/g) at 0.5 mole/L as shown in **Figure 4(c)**.

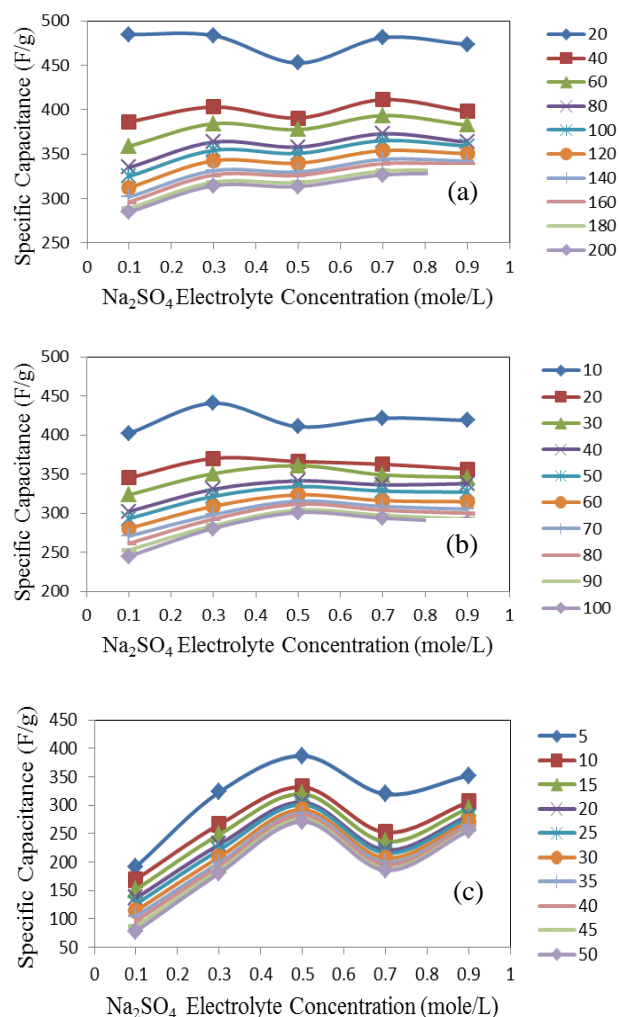


**Figure 4.** Variation of specific capacitance with  $\text{Na}_2\text{SO}_4$  electrolyte concentration for different mass loadings of electrode films: (a) 25 (b) 50, and (c)  $100 \mu\text{g}/\text{cm}^2$  at different actual currents 1 to 10 mA (the shown current values in plots are the corresponding's in A/g)

### 3.2. Cyclic Voltammetry (CV)

The cyclic voltammetry curves (CV) of potentiostatic anodically deposited  $\text{MnO}_2$  films at different mass loadings 25, 50, and  $100 \mu\text{g}/\text{cm}^2$  on etched SS electrodes were investigated in  $\text{Na}_2\text{SO}_4$  electrolyte solution of different concentrations 0.1, 0.3, 0.5, 0.7, and 0.9 mole/L at different applied voltage scan rates, from 10 mV/s to 100 mV/s, in the potential window range, from 0 to 1 V for each concentration. **Figure 5(a)-(c)** shows the CV plots at scan rate of 100 mV/s for tested concentrations at different mass loadings (a) 25, (b) 50, and (c)  $100 \mu\text{g}/\text{cm}^2$ . Those curves indicate that rectangular curves without redox peaks are obtained in the tested potential window, indicating the existing of a high capacitive behavior with a good response of ion (or charge carrier) transfer. However, the resistive like behavior obtained at high mass loading of  $100 \mu\text{g}/\text{cm}^2$  in low electrolyte concentration of 0.1 mole/L at scan rate of 100 mV/s, is related to the high resistance due to mass increase and decreasing number of electrolyte ions which is a

characteristic behavior of high mass loading of thin films.

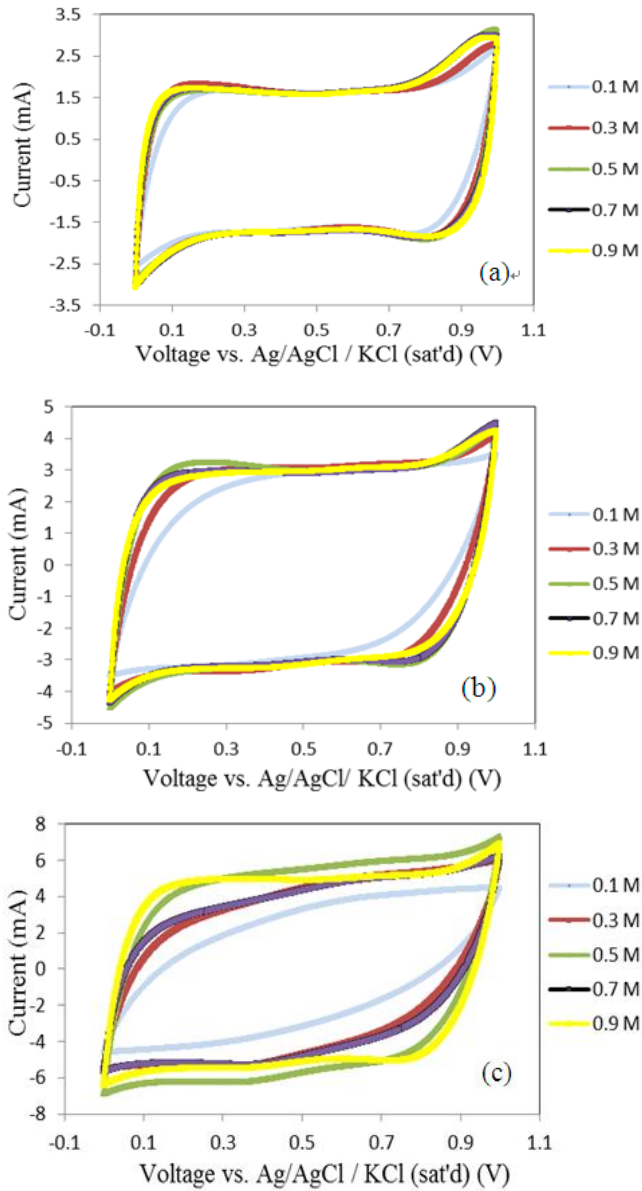


**Figure 5.** CV curves for deposited MnO<sub>2</sub> films at different mass loadings (a) 25 (b) 50, and (c) 100 µg/cm<sup>2</sup> at scan rate of 100 mV/s in different Na<sub>2</sub>SO<sub>4</sub> electrolyte concentrations of 0.1, 0.3, 0.5, 0.7, and 0.9 mole/L

Cyclic voltammetry is a simple but strong method of electrochemical analysis techniques that measures the current induced by a cell under test as function of the applied voltage. Among electrochemical techniques, CV is the most widely used to determine how charges behave at an electrode-electrolyte interface in a specific potential range [27]. In this technique, the potential of the working electrode is scanned back and forth at a constant rate ( $\Delta V/\Delta t$ ) in a potential window for several cycles. The resulted current values are plotted as a function of the applied voltage. CV is a very useful and simple tool to study the capacitance, particularly for electrical double layer capacitors (EDLCs) [28,29].

The titling of the voltammogram window toward the

vertical axis at higher scan rates for mass loading of 100 µg/cm<sup>2</sup> at low electrolyte concentration 0.1 mole/L, is attributed to the domination of the double layer storage process only at lower scan rates as presented in **Figure 6(c)**.

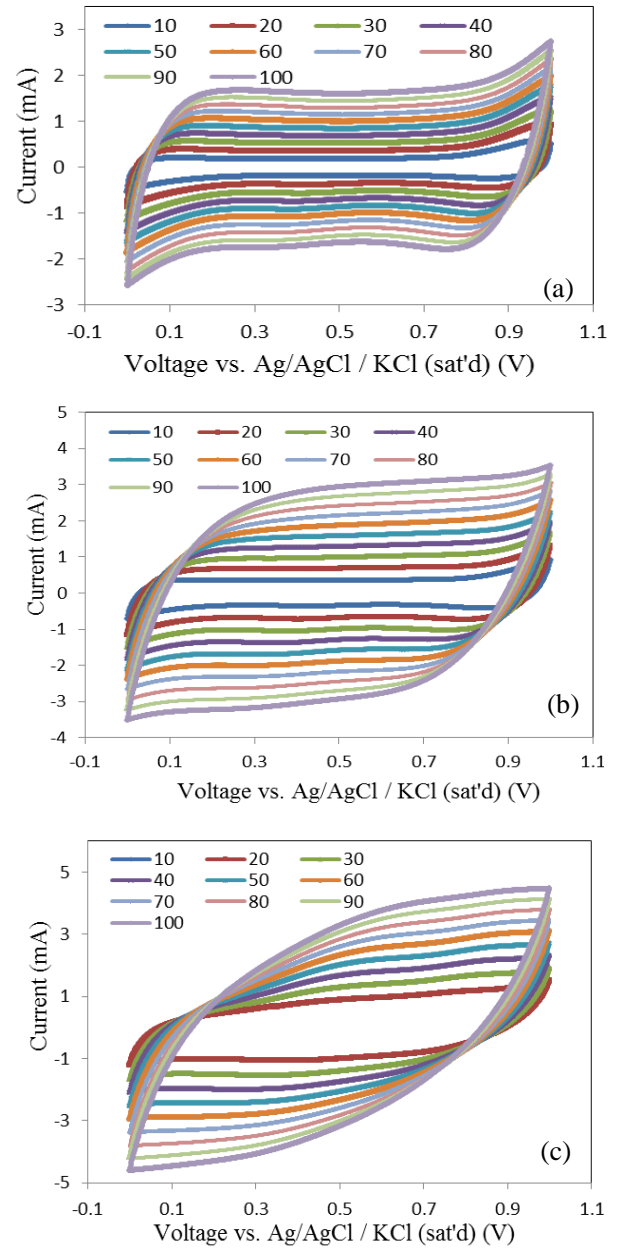


**Figure 6.** CV curves for deposited MnO<sub>2</sub> films at different mass loadings (a) 25 (b) 50, and (c) 100 µg/cm<sup>2</sup> at different scan rates (10-100 mV/s) in 0.1 mole/L concentration of Na<sub>2</sub>SO<sub>4</sub> electrolyte

The specific capacitance (SC) in F/g of the deposited film is given by the amount of capacitive charge, Q in coulombs (equals half the integrated area of the corresponding CV curve) presented in **Figure 5** and **Figure 6**, divided by the product of the film mass, m in grams times the width of the applied potential window,  $\Delta V$  in Volts, and is given by Equation (2)

$$SC = Q / (m \Delta V) \quad (2)$$

**Figure 7** investigates the dependence of the SC on the scan rate for electrodes with deposited films of mass loading  $25 \mu\text{g}/\text{cm}^2$ , and measured in different electrolyte concentrations. It is observed that the specific capacitance values of films for all electrolyte concentrations decrease as the scan rate increases. This observed behavior can be attributed to the high probability of ion insertion or accessibility into the voids of  $\text{MnO}_2$  lattice at low scan rate. The specific capacitance achieved at lower scan rate is the maximum utilization of the electrode material surface [26]. Also, for faradaic energy storage, at higher scan rate, electron transfer process is hindered because of depletion or saturation of the electrons in the electrolyte inside the electrode. This slow process of electron transfer inherently causes increase in resistivity and results in drop in the specific capacitance of the electrode. Furthermore, this fall in specific capacitance implies that the surface of the electrode material is not completely utilized for electron transfer at higher scan rates. It is well known that, at the same scan rate for a certain mass loading, as the integrated area of the CV curves increases, the higher the specific capacitance (SC) of the deposited film is obtained.

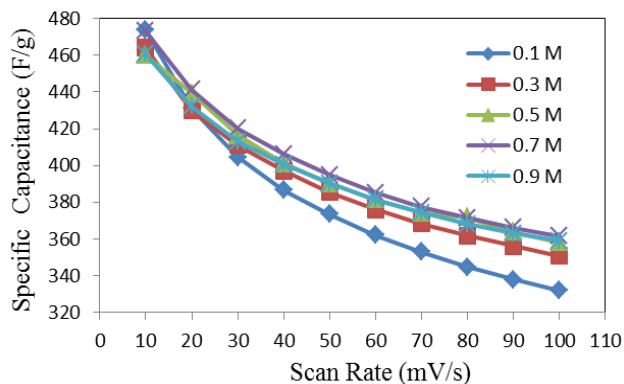


**Figure 7.** The variation of specific capacitance with scan rate for deposited  $\text{MnO}_2$  film at mass loading of  $25 \mu\text{g}/\text{cm}^2$ , as measured in different electrolyte concentrations of  $\text{Na}_2\text{SO}_4$

The higher specific capacitance values obtained at different concentration of  $\text{Na}_2\text{SO}_4$  electrolyte 0.1, 0.3, 0.5, 0.7 and 0.9 mole/L for electrodeposited films at mass loading of  $25 \mu\text{g}/\text{cm}^2$  and scan rate of 10 mV/s are 473.8, 464.2, 460.2, 473.2, and 460.6 F/g, respectively. The obtained specific capacitance values at scan rate of 100 mV/s are 332, 350.8, 358.2, 361.4, and 359 F/g, respectively. This is in coincidence with the galvanostatic charge-discharge results presented in **Figure 3**.

### 3.3. Impedance Spectroscopy Technique

In general, the power output capability of electrochemical supercapacitors, depend strongly on the rates of ionic mass transport and the equivalent series resistance (ESR) [30,31]. Electrochemical impedance spectroscopy (EIS) has been widely used to study the redox (charging/discharging) processes of electrode materials and to evaluate their electronic and ionic conductivities.

**Figure 8(a)** shows the obtained results of electrochemical impedance spectroscopy measurements, recorded in the frequency range of 10 mHz–100 kHz, under applying 10 mV amplitude at room temperature for the deposited mass  $25 \mu\text{g}/\text{cm}^2$  of  $\text{MnO}_2$  film. While **Figure 8(b)** represents a part of **Figure 8(a)** which is corresponding to lower values of both real and imaginary impedances of **Figure 8(a)** after being zoomed in.

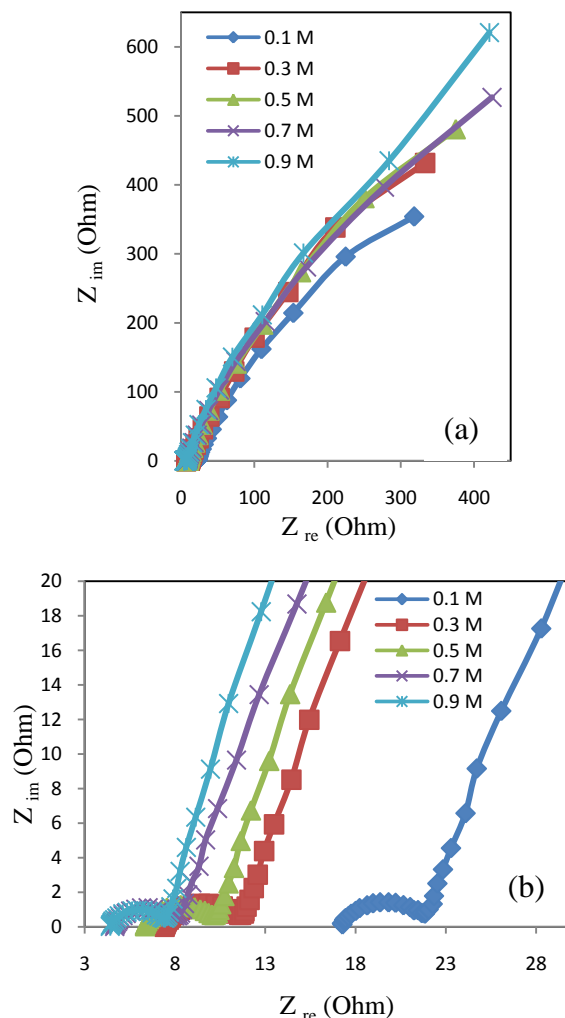


**Figure 8.** EIS plots for deposited mass loading of  $25 \mu\text{g}/\text{cm}^2$  for  $\text{MnO}_2$  films investigated in different concentrations of  $\text{Na}_2\text{SO}_4$  electrolyte in the frequency range of 10 mHz –100 kHz applying 10 mV amplitude

Inspection of **Figure 8(b)** reveals that the observed plots show different behaviors in the applied frequency range through the appearance of semi-circle at high frequency region and a linear behavior at low frequency regions, indicating both of the resistive and capacitive behaviors of the investigated electrode, respectively. In the high frequency region, there is an initial high frequency intercept of the semi-circle at the beginning with the real impedance axis corresponding to the equivalent series resistance (ESR), which is the sum of two major parts, an electronic resistance and an ionic one; it includes the ionic resistance of the electrolyte, interface resistance of the active material, resistance of the current collector, and the contact resistance

at electrode/electrolyte interface. The high frequency intercept is followed by a semicircle that is primarily due to the porous nature of electrode and the presence of resistance at electrode-electrolyte interface and corresponds to the charge transfer resistance ( $R_{ct}$ ) [2,32], i.e. interfacial reaction kinetics. The electrode possibly blocks the electron exchange of faradic process at the electrode/electrolyte interface. The value of  $R_{ct}$  can be derived from the diameter of the semicircle [30,32,33]. In the low frequency region, a linear region is obtained due to Warburg diffusion impedance, the beginning of the linear part represents the combination of resistive and capacitive behaviours of the ions penetrating into the electrode pores. As the frequency decreases, the capacitive behaviour dominates which results from the formation of the electric double layer system at the electrolyte/electrode interface; in this region, the ions can more easily diffuse into the micro-pores. The increasing slope trend of the line exhibits the capacitive nature related to the film charging mechanism that is the typical characteristic for porous electrodes. The associated parameters with bulk properties of electrolyte and electrode-electrolyte interface have been evaluated and listed in **Table 1**.

**Table 1.** Charge transfer resistance ( $R_{ct}$ ), equivalent series resistance (ESR) for tested PS deposited MnO<sub>2</sub> films at mass loading of 25  $\mu\text{g}/\text{cm}^2$  in different concentrations of Na<sub>2</sub>SO<sub>4</sub> electrolyte

Concentration (mole/L)	$R_{ct}$ (Ohm)	ESR (Ohm)
<b>0.1</b>	6.04	17.2
<b>0.3</b>	5.38	7.35
<b>0.5</b>	4.89	6.29
<b>0.7</b>	4.45	4.63
<b>0.9</b>	3.91	4.43

Referring to **Table 1** and fitting of Nyquist plots in **Figure 8**, for mass loading of 25  $\mu\text{g}/\text{cm}^2$ , the estimated ESR values decrease as the electrolyte concentration increases. This decrease in the ESR is due to the decrease in the ionic resistance of the electrolyte which is one of the ESR components. The optimized ESR values are 4.63 and 4.43  $\Omega$  at Na<sub>2</sub>SO<sub>4</sub> electrolyte concentration 0.7 and 0.9 mole/L, respectively. On the other hand, the estimated  $R_{ct}$  values decrease with the concentration increase. The general trend is an enhancement in the charge transfer resistance with increase of electrolyte concentration that reflects the improvement in the electronic and ionic conductivities of the electrode-electrolyte interface.

## 4. Conclusions

Three different mass loadings (25, 50 and 100  $\mu\text{g}/\text{cm}^2$ ) of MnO<sub>2</sub> films were anodically electrodeposited from 0.25 M manganese acetate solution by applying potentiostatic technique on 304-stainless steel current collector etched with 98% H<sub>2</sub>SO<sub>4</sub>. Effect of concentration of Na<sub>2</sub>SO<sub>4</sub> electrolyte solution (ranged from 0.1 to 0.9 M) on the capacitive behavior was studied and optimized. According to the electrochemical measurements, it was found that the highest

specific capacitances (484.7, 483.4 and 481.1 F/g) was obtained at current density of 20 A/g (or 0.5 mA/cm<sup>2</sup>) for MnO<sub>2</sub>/SS electrode with 25  $\mu\text{g}/\text{cm}^2$  mass loading at 0.1, 0.3 and 0.7 mole/L Na<sub>2</sub>SO<sub>4</sub> electrolyte concentration, respectively. This optimized capacitive behavior with the potentiostatically deposited MnO<sub>2</sub> film on 304-stainless steel current collector can be considered as a promising electrode for high energy storage supercapacitors.

## ACKNOWLEDGEMENTS

This work was financially supported by Science & Technology Development Fund (STDF), Egypt, Grant No 13855.

## REFERENCES

- [1] A.F. Burke, T.C. Murphy, D.H. Goughtly, B. Vyas, T. Takamura, and J. R. H. (Eds.), "Materials for electrochemical energy storage and conversion--batteries, capacitors, and fuel cells," Pittsburgh, Pa., 1995.
- [2] B. E. Conway, Electrochemical supercapacitors: scientific fundamentals and technological applications. New York [u.a.]: Plenum Press, 1999.
- [3] B. Pal, S. Yang, S. Ramesh, V. Thangadurai, and R. Jose, "Electrolyte selection for supercapacitive devices: a critical review," *Nanoscale Advances*, vol. 1, pp. 3807-3835, 2019.
- [4] G. A. M. Ali, M. M. Yusoff, Y. H. Ng, H. N. Lim, and K. F. Chong, "Potentiostatic and galvanostatic electrodeposition of manganese oxide for supercapacitor application: A comparison study," *Current Applied Physics*, vol. 15, pp. 1143-1147, 2015.
- [5] S. C. Pang, M. A. Anderson, and T. W. Chapman, "Novel Electrode Materials for Thin-Film Ultracapacitors: Comparison of Electrochemical Properties of Sol-Gel-Derived and Electrodeposited Manganese Dioxide," *Journal of The Electrochemical Society*, vol. 147, pp. 444-450, 2000.
- [6] D. Z. W. Tan, H. Cheng, S. T. Nguyen, and H. M. Duong, "Controlled synthesis of MnO<sub>2</sub>/CNT nanocomposites for supercapacitor applications," *Materials Technology*, vol. 29, pp. A107-A113, 2014.
- [7] M. Toupin, T. Brousse, and D. Bélanger, "Charge Storage Mechanism of MnO<sub>2</sub> Electrode Used in Aqueous Electrochemical Capacitor," *Chemistry of Materials*, vol. 16, pp. 3184-3190, 2004.
- [8] A. E. Fischer, K. A. Pettigrew, D. R. Rolison, R. M. Stroud, and J. W. Long, "Incorporation of Homogeneous, Nanoscale MnO<sub>2</sub> within Ultraporous Carbon Structures via Self-Limiting Electroless Deposition: Implications for Electrochemical Capacitors," *Nano Letters*, vol. 7, pp. 281-286, 2007.
- [9] G. Yu, L. Hu, M. Vosgueritchian, H. Wang, X. Xie, J. R. McDonough, X. Cui, Y. Cui, and Z. Bao, "Solution-Processed Graphene/MnO<sub>2</sub> Nanostructured

Textiles for High-Performance Electrochemical Capacitors," *Nano Letters*, vol. 11, pp. 2905-2911, 2011.

- [10] L. Hu, W. Chen, X. Xie, N. Liu, Y. Yang, H. Wu, Y. Yao, M. Pasta, H. N. Alshareef, and Y. Cui, "Symmetrical MnO<sub>2</sub>-Carbon Nanotube-Textile Nanostructures for Wearable Pseudocapacitors with High Mass Loading," *ACS Nano*, vol. 5, pp. 8904-8913, 2011.
- [11] L. Xingyou, H. Akihiko, F. Takeshi, and C. Mingwei, "Nanoporous metal/oxide hybrid electrodes for electrochemical supercapacitors," *Nature Nanotechnology*, vol. 6, pp. 232-236, 2011.
- [12] N. Nagarajan, M. Cheong, and I. Zhitomirsky, "Electrochemical capacitance of MnOx films," *Materials Chemistry and Physics*, vol. 103, pp. 47-53, 2007.
- [13] M. Toupin, T. Brousse, and D. Belanger, "Influence of Microstructure on the Charge Storage Properties of Chemically Synthesized Manganese Dioxide," *Chemistry of Materials*, vol. 14, pp. 3946-3952, 2002.
- [14] R. N. Reddy and R. G. Reddy, "Sol-gel MnO<sub>2</sub> as an electrode material for electrochemical capacitors," *Journal of power sources*, vol. 124, p. 330, 2004.
- [15] H. Y. Lee and J. B. Goodenough, "Supercapacitor Behavior with KCl Electrolyte," *Journal of Solid State Chemistry*, vol. 144, pp. 220-223, 1999.
- [16] V. Subramanian, H. Zhu, R. Vajtai, P. M. Ajayan, and B. Wei, "Hydrothermal Synthesis and Pseudocapacitance Properties of MnO<sub>2</sub> Nanostructures," *The Journal of Physical Chemistry B*, vol. 109, pp. 20207-20214, 2005.
- [17] T. Yousefi, A. N. Golikand, M. Hossein Mashhadizadeh, and M. Aghazadeh, "Facile synthesis of  $\alpha$ -MnO<sub>2</sub> one-dimensional (1D) nanostructure and energy storage ability studies," *Journal of Solid State Chemistry*, vol. 190, pp. 202-207, 2012.
- [18] C.-C. Hu and T.-W. Tsou, "Capacitive and textural characteristics of hydrous manganese oxide prepared by anodic deposition," *Electrochimica Acta*, vol. 47, pp. 3523-3532, 2002.
- [19] X. Hu, X. Lin, Z. Ling, Y. Li, and X. Fu, "Fabrication and Characteristics of Galvanostatic Electrodeposited MnO<sub>2</sub> on Porous Nickel from Etched Aluminium," *Electrochimica Acta*, vol. 138, pp. 132-138, 2014.
- [20] G. A. M. Ali, L. L. Tan, R. Jose, M. M. Yusoff, and K. F. Chong, "Electrochemical performance studies of MnO<sub>2</sub> nanoflowers recovered from spent battery," *Materials Research Bulletin*, vol. 60, pp. 5-9, 2014.
- [21] G. Yang, B. Wang, W. Guo, Z. Bu, C. Miao, T. Xue, and H. Li, "Liquid crystalline phase synthesis of nanoporous MnO<sub>2</sub> thin film arrays as an electrode material for electrochemical capacitors," *Materials Research Bulletin*, vol. 47, pp. 3120-3123, 2012.
- [22] G. M. Jacob and I. Zhitomirsky, "Microstructure and properties of manganese dioxide films prepared by electrodeposition," *Applied Surface Science*, vol. 254, pp. 6671-6676, 2008/08.
- [23] M. Gupta, D. Pinisetty, J. C. Flake, and J. J. Spivey, "Pulse Electrodeposition of Cu-ZnO and Mn-Cu-ZnO Nanowires," *Journal of The Electrochemical Society*, vol. 157, pp. D473-D478, 2010.
- [24] J. Wu, C. D. Johnson, Y. Jiang, R. S. Gemmen, and X. Liu, "Pulse plating of Mn-Co alloys for SOFC interconnect applications," *Electrochimica Acta*, vol. 54, pp. 793-800, 2008.
- [25] J. Wang, Y. Xu, J. Wang, X. Du, F. Xiao, and J. Li, "High charge/discharge rate polypyrrole films prepared by pulse current polymerization," *Synthetic Metals*, vol. 160, pp. 1826-1831, 2010.
- [26] A. K. Mishra and S. Ramaprabhu, "Functionalized Graphene-Based Nanocomposites for Supercapacitor Application," *The Journal of Physical Chemistry C*, vol. 115, pp. 14006-14013, 2011.
- [27] W. Vielstich. (2010). *Handbook of fuel cells: fundamentals, technology, and applications*. Available: <http://dx.doi.org/10.1002/9780470974001>.
- [28] T. Tevi, H. Yaghoubi, J. Wang, and A. Takshi, "Application of poly (p-phenylene oxide) as blocking layer to reduce self-discharge in supercapacitors," *POWER Journal of Power Sources*, vol. 241, pp. 589-596, 2013.
- [29] T. Tevi, S. W. Saint Birch, S. W. Thomas, and A. Takshi, "Effect of Triton X-100 on the double layer capacitance and conductivity of poly(3,4-ethylenedioxythiophene): poly(styrenesulfonate) (PEDOT:PSS) films," *Synthetic Metals*, vol. 191, pp. 59-65, 2014.
- [30] A. Izadi-Najafabadi, D. T. H. Tan, and J. D. Madden, "Towards High Power Polypyrrole/Carbon Capacitors," *Synthetic Metals*, vol. 152, pp. 129-132, 2005.
- [31] A. Celzard, F. Collas, J. F. Maréché, G. Furdin, and I. Rey, "Porous electrodes-based double-layer supercapacitors: pore structure versus series resistance," *Journal of Power Sources*, vol. 108, pp. 153-162, 2002.
- [32] S. Hassan, M. Suzuki, and A. Abd El-Moneim, "Capacitive Behavior of Manganese Dioxide/Stainless Steel Electrodes at Different Deposition Currents," *MATERIALS American Journal of Materials Science*, vol. 2, pp. 11-14, 2012.
- [33] F. Xiao and Y. Xu, "Pulse electrodeposition of manganese oxide for high-rate capability supercapacitors," *Int.J. Electrochem. Sci. International Journal of Electrochemical Science*, vol. 7, pp. 7440-7450, 2012.